Carbohydrate Polymers 175 (2017) 370–376

Contents lists available at ScienceDirect

Carbohydrate Polymers

journal homepage: www.elsevier.com/locate/carbpol

Research Paper

Cellulose nanocrystals from passion fruit peels waste as antibiotic drug carrier

Christian J. Wijaya [a], Stephanie N. Saputra [a], Felycia E. Soetaredjo [a], Jindrayani N. Putro [b], Chun X. Lin [c], Alfin Kurniawan [b], Yi-Hsu Ju [b,*], Suryadi Ismadji [a,*]

[a] Department of Chemical Engineering, Widya Mandala Surabaya Catholic University, Kalijudan 37, Surabaya 60114, Indonesia
[b] Department of Chemical Engineering, National Taiwan University of Science and Technology, Taiwan
[c] The University of Queensland, St. Lucia, Qld 4072, Brisbane, Australia

ARTICLE INFO

Article history:
Received 25 March 2017
Received in revised form 23 July 2017
Accepted 1 August 2017
Available online 4 August 2017

Keywords:
Cellulose nanocrystals
Passionfruit peel
Cellulose
Drug release

ABSTRACT

Due to its excellent chemical and physical properties, cellulose nanocrystals (CNC) possess many potential advanced functional applications. In this study, CNC was extracted from natural product by hydrolyzing cellulose segment of passionfruit peels using sulphuric acid solution. The capability of CNC as drug carrier was tested toward tetracycline antibiotic. The drug loading processes were carried out at various pH (3–7) with the optimum uptake of tetracycline achieved at pH 3. The *in vitro* release of tetracycline drug was carried out in phosphoric buffer medium with two different pH conditions at 37 °C. The highest release of tetracycline (82.21%) was achieved at pH 7.2, while the lowest one (25.1%) was achieved at pH 2.1, where the release pattern follow a second order kinetic model. This study highlight the potential application of CNC derived from natural resources as drug carrier without harmful chemical excipients that comply with health safety, biocompatible, biodegradable.

1. Introduction

Cellulose nanocrystals (CNC) is a unique biopolymeric material with nanometers size and possesses a crystal structure. Generally, CNC has crystal structure of needle or rod like with 5–30 nm diameter size and 100 nm to several micrometers length. CNC has better physical and chemical characteristics than its precursor for example higher surface area, reactive hydroxyl group in the surface, biocompatible, etc. (Lin & Dufresne, 2014). Due to its superior properties, CNC is suitable for many advanced functional applications such as tissue engineering, drug delivery, reinforcement of composite materials, template for nanomaterial synthesis, protein or enzyme immobilization, emulsion stabilizer, etc. (Sarma, Ayadi, Brar, & Berry, 2017; Qing et al., 2016; Sun, Hou, He, Liu & Ni, 2014).

Various kind of lignocellulosic biomass have been reported as the raw materials to produce CNC for example pineapple leaf fibers (Cherian et al., 2010), sugarcane bagasse (Mandal & Chakrabarty, 2011), oil palm residue (Haafiz, Eichhorn, Hassan & Jawaid, 2013), chardonnay grape skins (Lu & Hsieh, 2012), groundnut shell (Bano & Negi, 2017), apple tree pruning, pea stalks (Garcia, Labidi, Belgacem & Bras, 2017), coconut fiber (Nascimento et al., 2016), cotton stalks (Shamskar, Heidari & Rashidi, 2016), rice husk (Barana, Salanti, Orlandi, Ali & Zoia, 2016), corncob (Silvério, Flauzino, Dantas & Pasquini, 2013; Ditzel et al., 2017Ditzel, Prestes, Carvalho, Demiate & Pinheiro, 2017Silvério, Flauzino, Dantas & Pasquini, 2013; Ditzel et al., 2017Ditzel, Prestes, Carvalho, Demiate & Pinheiro, 2017Silvério et al., 2013Silvério, Flauzino, Dantas & Pasquini, 2013; Ditzel et al., 2017Ditzel, Prestes, Carvalho, Demiate & Pinheiro, 2017). In this study, passionfruit peels with high content of crystalline cellulose fragments (58.1%) are used as the precursor to generate high yield of CNC, which to the best of our knowledge has not been reported elsewhere. Passionfruit is usually cultivated in tropical and subtropical area, such as Indonesia with a large production capacity reaching over 180 kilotons in 2015, and this production rate is keep increasing each year. Most of the passionfruit is utilized as the feedstock of beverage industries that generate about 30 – 40% of biomass in South Sulawesi as the main producer of passionfruit in Indonesia. So far, these passionfruit peels have not been used by any manufacturing industry except for fertilizing purpose, hence, the utilization of passionfruit peels as an alternative precursor to fabricate CNC will add significant value to passionfruit growers.

One important aspect in CNC applications is the usage of CNC as drug carrier that can offer some benefits such as good bio-

* Corresponding authors.
E-mail addresses: yhju@mail.ntust.edu (Y.-H. Ju), suryadiismadji@yahoo.com, alfin_kur@yahoo.com (S. Ismadji).

http://dx.doi.org/10.1016/j.carbpol.2017.08.004
0144-8617/

compatibility, non-toxic and biodegradable as reported by many researchers (Jackson et al., 2011; Qing et al., 2016; Zainuddin, Ahmad, Kargarzadeh & Ramli, 2017). However, the main disadvantage of using CNC as drug carrier is it has low drug loading capability toward certain hydrophobic drugs. Chemical modification of CNC through the hydroxyl groups of its glucose units using cationic surfactants such as cetyltrimethylammonium bromide (CTAB) is normally done to increase the adsorption capacity of CNC towards hydrophobic drugs, (Lam, Male, Chong, Leung & Luong, 2012). Qing et al. (2016). It is suggested that CTAB coated CNC have good affinity towards water insoluble anticancer drugs. CTAB was also employed for CNC modification to bind a significant amount of curcumin as reported by Zainuddin, Ahmad, Kargarzadeh and Ramli (2017). The modification of CNC with CTAB is undeniably can increase drugs uptake, including the uptake of tetracycline (Jakson et al., 2011); however, health and safety issues of drug excipients need to put into consideration when designing drug carrier. As a cationic surfactant, CTAB may potentially bring acute and chronic effects towards human health and aquatic organisms, where it can cause serious damage to eyes, irritating to respiratory system and skin, and long-term adverse effects in the aquatic environment (Sigma-Aldrich, 2013). This paper describes the utilization of unmodified CNC from natural resources of passionfruit peels as the drug carrier of antibiotic tetracycline with high adsorption capacity achieved through pH adjustment. The main advantage of using CNC as potential candidate for tetracycline carrier compared to the existing system is the release of tetracycline can be controlled so the absorption of tetracycline in the human body is much more efficient.

2. Experimental

2.1. Materials

Passionfruit peels (PP) was obtained from passionfruit syrup industry in Makassar, South Sulawesi, Indonesia. PP was repeatedlywashed and subsequently dried under the sunlight for three days. Dried PP was then pulverized and sieved through a 140-mesh screen to become PP powder. Sodium hydroxide, hydrogen peroxide, sulphuric acid, and tetracycline hydrochloride antibiotic were purchased as an analytical grade from Sigma-Aldrich (Singapore). The dialysis tubes used in this study was obtained from Spectrum Laboratories, Inc., and has MWCO 12–14 kD. The dialysis membrane or tube was manufactured from natural cellulose reconstituted from cotton liners.

2.2. Preparation of CNC

The extraction of PP was carried out according to the following procedures: For delignification step, 50 g of PP powder was treated using 500 mL of 2 M sodium hydroxide solution at 80 °C for 4 h with constant stirring. Subsequently, the solid product was separated from the solution and washed with distilled water for several times (4–5 times) and dried at 50 °C for 12 h. For bleaching step, the dried and delignified PP was treated using sodium hydroxide (4% w/v) and hydrogen peroxide solution (50%) with the ratio of 1:1 (v/v). The delignified PP was immersed in sodium hydroxide solution, and heated at 50 °C under constant stirring, and then the hydrogen peroxide was added to the mixture dropwise. When all of the hydrogen peroxide has been added to the mixture, the bleaching process was continued for another 60 min under continuous stirring at 50 °C. After the bleaching process was completed, the solid portion was separated from the liquid by centrifugation and repeatedly washed with reverse osmosis water until the washing solution reached a neutral t pH and the solid was dried at 50 °C in an oven for 24 h.

The preparation of CNC from the PP was carried out using sulphuric acid hydrolysis process. The concentration of the sulphuric acid used in this study was 52% (8.4 M), and the hydrolysis process was conducted at 50 °C for 60 mins, with solid to acid ratio of 1:10 (w/w). In the preliminary experiment, the influence of sulphuric acid concentration on the yield of CNC was studied, and the use of sulphuric acid with concentration of 52% (8.4 M) gave the highest yield of CNC. At temperature higher than 50 °C, some of the CNC were further hydrolyzed to sugar. While, at temperature lower than 50 °C, the extraction of CNC from cellulose proceed at slower rate of extraction, and produce lower yield of CNC. After 60 mins hydrolysis time, the reaction was stopped by adding an excess amount of cold reverse osmosis water (4 °C) to the system. Subsequently, the suspension was centrifuged at 6000 rpm for 5 min. The turbid supernatant was collected and placed in dialysis tubes for three days (every 8 h, the dialysis water was replaced with fresh reverse osmosis water), then freeze-dried to obtain the CNC. Freeze drying process was carried out using manifold method. The freeze dryer (Labconco) was operated at temperature of −42 °C and pressure of 0.08 mbar.

2.3. Characterization

The chemical composition (moisture content, lignin, hemicellulose, cellulose, and ash) of PP before and after the extraction process was determined by TGA method (Carrier et al., 2011).

To obtain a complete information about the characteristic of CNC extracted from PP, the CNC was characterized using Scanning Electron Microscopy (SEM), X-ray Diffraction (XRD), FTIR, Zeta Potential Analyzer, and thermal gravimetric analysis (TGA). The SEM analysis was used to observe the morphology of the CNC using a JEOL JSM-6390 field emission SEM operated at an accelerating voltage of 5 kV. Before the SEM analysis was carried out, the CNC samples were coated with a thin layer of conductive platinum using a fine auto coater (JFC-1200, JEOL, Ltd., Japan) for 120 s in an argon atmosphere.

The XRD analysis was carried out to investigate the crystallinity of CNC using a Philips PANalytical X'Pert powder X-ray diffractometer with a monochromated high-intensity Cu $K\alpha_1$ radiation ($\lambda = 0.15406$ nm). The diffractograms were obtained at 40 kV, 30 mA and a step size of 0.05°/s. FTIR analysis of CNC samples were conducted using FTIR Shimadzu 8400S with KBr pelleting method. The FTIR spectrum of CNC was recorded at the wavenumber range of 4000–500 cm^{-1}. The surface charge of CNC was measured at different pH using Zeta Potential Analyzer (NanoBrook ZetaPal). The zeta potential measurement was conducted at 25 °C. The concentration of the CNC sample was 0.01%. Sodium chloride was added to the sample to maintain the ionic strength of the solution at 0.0001 mol/L. The viscosity of the sample was measured by viscometer (Brookfield DV2T), and this viscosity value (0.931 cP) was used as a key parameter for zeta potential measurement. The particle size of CNC was measured using zeta sizer (NanoBrook ZetaPal). Measurement parameters for CNC particle size are as follow: temperature = 25 °C, liquid = water, viscosity = 0.890 cp, refractive index of fluid = 1.330, angle = 90.0 and wavelength = 659 nm. ZetaPals particle sizing software Ver. 5.34 was used for the calculation of particle size distribution. The thermal gravimetric analysis was employed to determine the thermal stability of CNC using a Perkin Elmer Diamond TG/DTA thermal analyzer with heating and cooling rate of 10 °C/min in continuous nitrogen gas flow of 150 mL min^{-1}. Bulk density of CNC was measured using a pycnometer, and the bulk density was obtained by division of weight of the CNC with volume occupied by the CNC. Five independent measurements were conducted and the mean value was taken as bulk density of CNC. The bulk density of CNC obtained by this method was 0.673 g/cm^3.

2.4. Adsorption of tetracycline

The adsorption study of tetracycline onto CNC was conducted isothermally at 30 °C under static condition at varied pH (3, 4, 5, 6, and 7). The adsorption study was carried out according to the following procedure: a known amount of CNC (0.01–0.5 gram) was added to a series of Erlenmeyer flasks containing 50 mL of solution with initial tetracycline concentration of 250 mg/L. All flasks were placed in Memmert type WB-14 thermostatic water bath shaker until the equilibrium time was reached (12 h). During the adsorption process, the temperature of the system was set at 30 °C. The CNC was separated from the solution by centrifugation. The initial (C_o) and equilibrium (C_e) concentrations of tetracycline in the solution were measured using Shimadzu UV/VIS-1700 Pharma Spectrophotometer at the maximum wavelength (610 nm). The amount of tetracycline adsorbed by CNC at equilibrium condition (q_e) was calculated by the following equation:

$$q_e = \frac{(C_o - C_e)}{m} V \quad (1)$$

Where m and V are the mass of CNC and the volume of solution, respectively. The adsorption studies were conducted in three independent experiments.

2.5. Tetracycline release study

The *in vitro* drug release study was carried out at 37 °C in PB (phosphoric buffer) mediums with two different pH of 7.2 and 2.1. A known amount of tetracycline loaded CNC (0.1 g) was added to a series of Erlenmeyer flasks containing 50 mL of phosphoric buffer solution. All flasks were placed in Memmert type WB-14 thermostatic water bath shaker and the temperature of the water bath was adjusted at 37 °C. During the drug release process, the Erlenmeyer flasks were shaken at 200 RPM. At certain interval of time, one by one of the Erlenmeyer flask was taken from the system; and the released concentration of tetracycline as a function of time (C_t) was analyzed using Shimadzu UV/VIS-1700 Pharma Spectrophotometer with initial drug loading in CNC at 121.5 mg/g determined through UV analysis. Phosphate buffer solution was employed as blank solution for UV analysis. Drug release studies were conducted in three independent experiments.

3. Result and discussion

3.1. Characteristics of CNC produced from passion fruit peels waste

TGA analysis was carried out to investigate the chemical compositions of dried PP before and after delignification process. The evaporation of free moisture content and bound water from the samples was observed at a temperature range from 50 °C to 200 °C. The thermal decomposition of hemicellulose occurred between 200 °C to 300 °C, while the disintegration of cellulose into lower molecular weight compounds occurred between 300 °C to 360 °C and lignin was decomposed at 360 °C to 500 °C. The chemical compositions of PP and its delignified form are summarized in Table 1. It shows the reduction of hemicellulose and lignin content after delignification process, which demonstrate that the pre-treatment process using sodium hydroxide (delignification), could effectively remove lignin and hemicellulose from PP.

The yield of CNC based on dry cellulose of PP is 58.1 ± 1.7% (sulphuric acid concentration of 52% (8.4 M), the temperature of hydrolysis was 50 °C, solid to the acid ratio 1:10, and hydrolysis time of 60 min). This high yield indicates that the cellulose fraction of PP contains more crystalline region than amorphous ones. During the hydrolysis process using sulphuric acid, the amorphous region of cellulose fibers was disintegrated into glucose and the crystalline part remained intact due to its excellent stability in sulphuric acid environment as evidenced through our observations below.

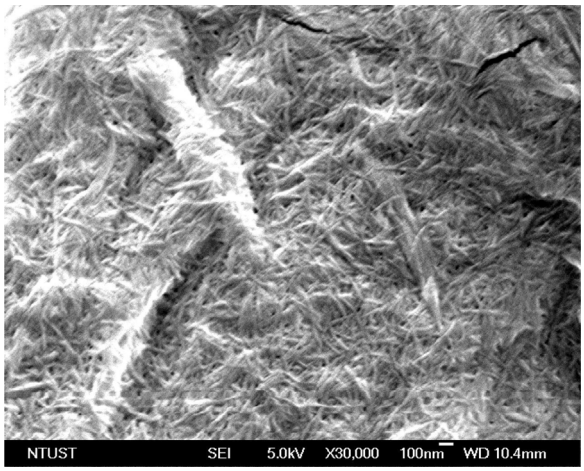

Fig. 1. SEM picture of CNC.

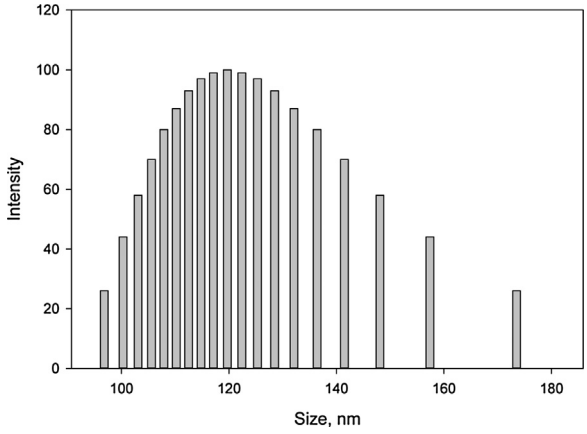

Fig. 2. Particle size distribution of CNC.

Fig. 1 shows the surface topography of CNC produced from PP. From this SEM observation, it can be seen that the CNC has rod-like morphology. As mentioned previously, this rod-like morphology is typical for CNC. The particle size distribution of CNC is given in Fig. 2.

The particle size of CNC from PP are around 103–173.5 nm with median size 139.7 nm and mean size 145.4 nm.

The X-ray diffraction (XRD) pattern of CNC from PP as well as the cellulose I standard crystal from JCPDS No. 00-050-22411 are depicted by Fig. 3 for comparison purpose. The XRD pattern of CNC shows four distinct peaks at 2θ = 15.5°, 16.4°, 22.8°, and 35°, which correspond to the $1\tilde{1}0$, 110, 200, and 004 planes. These peaks are located in similar position as the peaks of cellulose I standard crystal, 15.9° ($1\tilde{1}0$), 16.4° (110), 22.6° (200), and 34.6° (004).

The crystallinity index of CNC was calculated by the following equation (Ditzel, Prestes, Carvalho, Demiate & Pinheiro, 2017):

$$\mathrm{CrI} = [1-(I_{am}/I_{200})]\mathrm{x}100\% \quad (2)$$

Where I_{am} is the minimum intensity between 110 and 200 lattices diffraction, while I_{200} is the maximum intensity of 200 lattice. I_{am} indicates the amorphous fraction of the cellulose, while I_{200} represents both of amorphous and crystalline regions of the cellulose. It is found that the crystallinity index (CrI) of CNC extracted from PP was 77.96%, which is similar to CNC from corncob (CrI = 78%)

Table 1
Chemical composition of passion fruit peels waste and its delignified form.

Component	Passion fruit peels waste (% wt.)	Delignified passion fruit peels waste (% wt.)	TGA temperature (°C)
Water	6.52	5.77	50–200
Hemicellulose	23.01	2.85	200–300
Lignin	36.18	2.27	300–360
Cellulose	28.58	79.64	360–500
Ash + carbon	5.71	9.47	>500

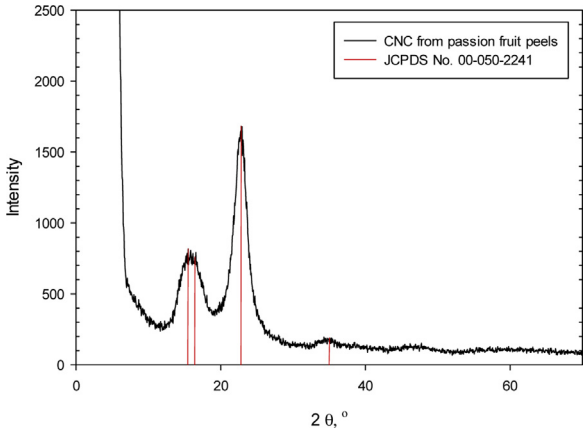

Fig. 3. The XRD spectrum of CNC from passion fruit peels waste.

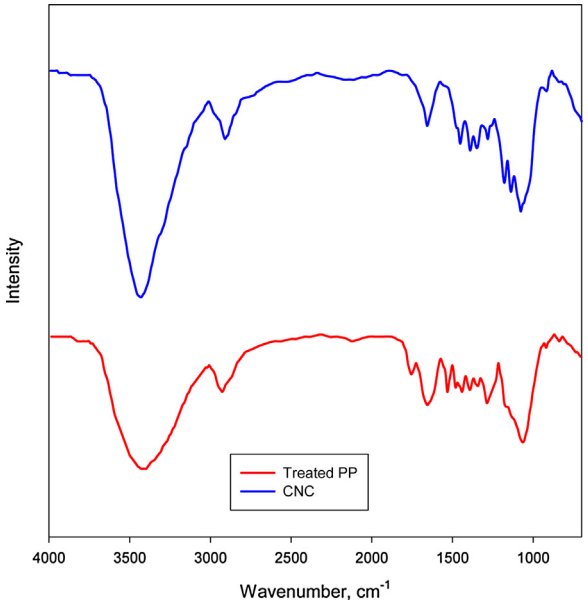

Fig. 4. FTIR spectra of passion fruit peels and CNC.

(Silvério et al., 2013), however it is higher than the (CrI) of CNC from mulberry (73.4%) (Li et al., 2009) and balsa wood (62.0-%) (Morelli, Marconcini, Pereira, Bretas & Branciforti, 2012).

The FTIR spectra of dried treated PP and CNC are depicted in Fig. 4, which show the following stretching bands located at 3418 cm^{-1} (OH), 2922 cm^{-1} (C—H), 1423 cm^{-1} (symmetric CH_2), 1376 cm^{-1} (CH), 1159 cm^{-1} (non-symmetric bridge C—O—C), 1066 cm^{-1} (skeletal vibrations C—O), 890 cm^{-1} (non-symmetric out-phase ring). The cellulose structure of PP contains more ordered structure than disordered structure as indicated by narrow absorption wavenumber between 1423 cm^{-1} and 890 cm^{-1} (Bano & Negi, 2017). This evidence confirms the high yield of CNC as mentioned above. Cellulose fibers consist of amorphous part and crystalline part. Amorphous part has disordered structure, while the crystalline part possesses ordered structured. In the acid hydrolysis process, the amorphous part of cellulose fibers will be hydrolyzed into glucose, whereas the crystalline fragments remain intact due to its excellent stability in acidic condition (Brinchi, Cotana, Fortunati, & Kenny, 2013). If the cellulose structure contains more ordered structure, so more CNC will be obtained. For industrial application, the cellulose with more ordered structure is much more desirable since it will give higher yield of CNC.

Naturally lignin has much more complex structure than cellulose, since it possesses phenolic hydroxyl groups, carbonyl groups, aliphatic hydroxyl groups, methoxyl groups, benzyl alcohol groups, and some terminal aldehyde groups (Todorciuc, Capraru, Kratochvilova & Popa, 2009). Some of the FTIR spectra bands of lignin content in the PP are located at 3436 cm^{-1} (hydroxyl groups in phenolic and aliphatic structures), 2932 cm^{-1} (CH stretching in aromatic methoxyl groups and methyl – methylene groups of the side chains), 1525 cm^{-1} (C—H asymmetric deformation in CH_2 and CH_3), 1424 cm^{-1} (C—O stretch in lignin, C—O linkage in guaiacyl aromatic methoxyl groups), 1351 cm^{-1} (syringyl ring breathing with C—O stretching), 1328 cm^{-1} (aromatic Cassionfruit peels (PP) can serve as potentialH in-plane deformation, typical of guaiacyl units), 1282 cm^{-1} (aromatic C—H in-plane deformation, typical of S units, with secondary alcohols and C=O stretching), 1222 cm^{-1} (C—O deformation in secondary alcohols and aliphatic ethers), and 1076 cm^{-1} (deformation vibrations of the C—O bands in primary alcohols) (Todorciuc et al., 2009). For hemicellulose content in PP, several FTIR stetching bands are located at 1754 cm^{-1} (free ester) (), 1731 cm^{-1} 1 (ketone/aldehyde C = O) (), 1443 cm^{-1} (O – H), 1373 cm^{-1} (C—H), and 929 cm^{-1} (glycosidic units) (Sim, Mohamed, Lu, Sarman & Samsudin, 2012).

Fig. 4 clearly shows that the CNC has sharp and intense absorption band at 3427 cm^{-1} (OH stretching bond for cellulose), where the shift of this absorption band from 3418 cm^{-1} to 3427 cm^{-1} is strongly associated with disruption of hydrogen bonding due to the removal of non-cellulosic fractions (Bano & Negi, 2017). CNC shows some similar characteristic stretching bands like cellulose I (the reference sample) as indicated by absorption bands at 1451 cm^{-1}, 1071 cm^{-1}, and 883 cm^{-1}. A new peak appears for CNC in 1402 cm^{-1} spectrum, which indicates the presence of sulfate esters (Coates, 2006) due to sulfuric acid hydrolysis.

The surface charge of CNC was measured at different pH. The surface charge of CNC is independent of pH and its value remains constant around −25 to −22 mV. This negative surface charge indicates that the CNC produced from PP can serve as effective adsorbent to adsorb cationic molecules in the solution.

Thermal decomposition properties of the CNC was determined through TGA and DTG methods as shown in Fig. 5. The initial weight loss in the temperature region of 35–200 °C correspond to the evaporation of free moisture content and bound water. Thermal degradation of CNC occurred at the temperature range of 215 °C to 353 °C associated with dehydration and depolymerization processes of cellulose. The optimum degradation temperature of CNC was at 303.4 °C. Further carbonization of intermediate char within N2 atmosphere occurred at temperature above 353 °C.

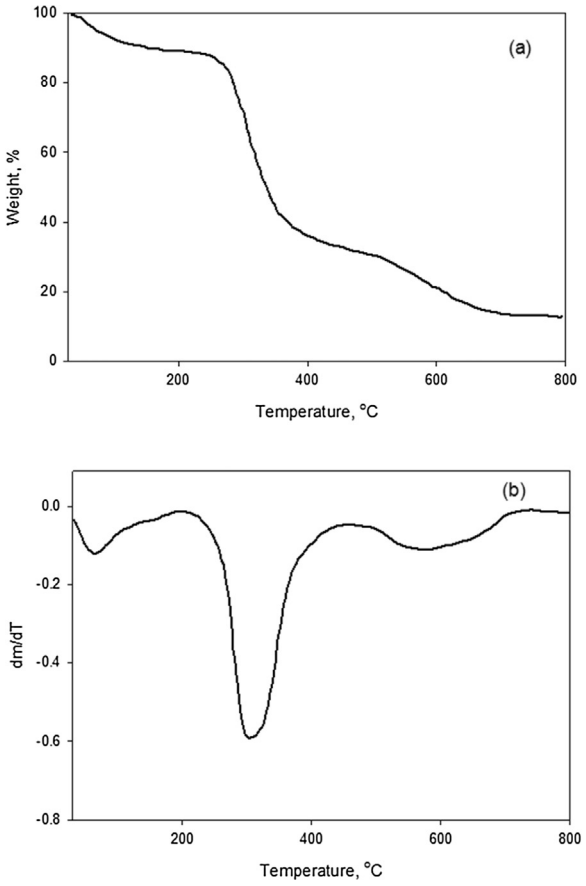

Fig. 5. TGA and DTG curves of CNC.

3.2. Adsorption of tetracycline

The adsorption of tetracycline on CNC sample was carried out at 30 °C in varied pH condition (3, 4, 5, 6, and7). Tetracycline is a pH dependent amphoteric antibiotic that may exists in three protonated functional groups: tricarbonyl methane group, phenolic deketone group, and dimethylamino group depending on the pH environment (Yu, Ma & Han, 2014). The tetracycline molecules present as cations at pH < 3.3, as zwitterions at pH between 3.3–7.7, and as anions at pH > 7.7 (Lin, Qiao, Yu, Ismadji & Lu, 2009; Yu, Ma & Han, 2014).

Langmuir and Freundlich adsorption equations were applied to fit the adsorption experimental data. Langmuir equation is presented as follow:

$$q_e = q_{max}\frac{K_L C_e}{(1 + K_L C_e)} \quad (3)$$

where q_{max} and K_L represents the adsorption capacity and the adsorption affinity of adsorbent, respectively

Freundlich equation is an empirical formula that is widely used to represent the liquid phase adsorption on the heterogeneous surface. The mathematical formula of Freundlich equation is presented as follows:

$$q_e = K_F C_e^{1/n} \quad (4)$$

where K_F represents the adsorption capacity and n the heterogeneity of the system with the value between 1–10. The higher the value of n, the more heterogeneous the system.

The adsorption isotherms of tetracycline on CNC at various pH are shown at Fig. 6. The colorful spherical symbols represent the experimental adsorption data, while the solid line and dash line represent the Langmuir and Freundlich theoretical values,

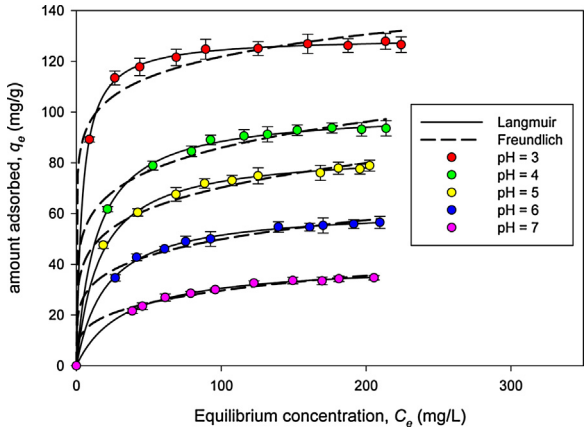

Fig. 6. Adsorption isotherm of tetracycline onto CNC.

respectively. This figure clearly shows that the pH condition play a significant role in the adsorption of tetracycline on CNC. The maximum loading amount of tetracycline was achieved at pH 3 as shown by Fig. 6.

This is consistent with the fact that tetracycline molecules behave as cations (positively charged) below pH 3.3, while the CNC surface was negatively charged, thus facilitate the electrostatic interaction between CNC surface (hydroxyl group and sulfate ester groups) and protonated tetracycline molecules as given in the following reaction mechanism

$$R\text{-}OH^- + C_{20}NH_{18}O_8\text{-}NH(CH_3)_2^+ \leftrightarrow C_{20}NH_{18}O_8\text{-}NH(CH_3)_2OH\text{-}R \quad (5)$$

$$R\text{-}S\text{-}O_3^- + C_{20}NH_{18}O_8\text{—}NH(CH_3)_2^+ \leftrightarrow C_{20}NH_{18}O_8\text{—}NH(CH_3)_2O_3\text{-}S\text{-}R \quad (6)$$

This electrostatic interaction leading to an optimum uptake of tetracycline by the CNC as much as 129.46 mg/g (Table 2). When the pH of the medium was increased to 4, 5, 6 and 7, the tetracycline molecules behave as zwitterions (having no net electrical charges), which led to a weak interaction between tetracycline and CNC surface that gradually decrease the adsorption amount of tetracycline to 40.43 mg/g (Table 2). Furthermore, hydrophobic interaction between the CNC surface and tetracycline decreased as the pH increased. The increase of pH of the solution increased the hydrophilicity of tetracycline (Yu et al., 2014Yu, Ma & Han, 2014). All of these phenomena causing the reduction of adsorption ability of CNC toward tetracycline molecules.

The parameters of Langmuir and Freundlich equations obtained from experimental data fitting with the models are summarized in Table 2. Both Fig. 6 and Table 2 confirm that the Langmuir equation can better fit into the experimental data than Freundlich equation. Now we will discuss the meaning of each parameter in Langmuir equation and compare it to the adsorption phenomena occurred during the adsorption of tetracycline on CNC. Parameter q_{max} in Langmuir equation represents the maximum adsorption capacity of CNC towards tetracycline molecules. The highest adsorption capacity was achieved at pH 3 as described above as shown by Fig. 6 and Table 2 However, with the increasing pH the adsorption capacity of CNC is decreasing, and this phenomenon is well represented by parameter q_{max} (Table 2). Parameter K_L represents the adsorption affinity, which indicates the strength of adsorbate attachment to the adsorbent. The higher the value of K_L, the stronger the attachment to the surface of the adsorbent that lead to more adsorbate adsorbed on the adsorbate surface. One of the primary mechanisms that control the adsorption of tetracycline on CNC at pH 3 was the electrostatic interaction. With the increase of pH, the electrostatic interaction was no longer serve as the controlling factor, instead the van der Waals force that play the role for weaker interaction between tetracycline molecules and the CNC. The value of parameter K_L decrease with the increase of the solution pH (Table 2), which

Table 2
Parameters of Langmuir and Freundlich for the adsorption of tetracycline onto CNC.

pH	Langmuir			Freundlich		
	q_{max} (mg/g)	K_L (L/mg)	R^2	K_F(mg/g)(L/mg)$^{-n}$	n	R^2
3	129.46	0.2494	0.998	76.89	10	0.982
4	100.45	0.0734	0.998	40.54	6.13	0.989
5	84.31	0.0621	0.997	29.87	5.38	0.992
6	61.86	0.0494	0.998	19.56	4.92	0.991
7	40.43	0.0307	0.997	8.88	3.82	0.991

Table 3
Tetracycline release efficiency of several drug carriers.

Drug carrier	Condition of drug release	Release profile	Efficiency, %	Reference
Cellulose nano crystal	pH 7.2 in PBS solution at temperature of 37 °C	Rapid release in the first 10 h (≈80%) and follow by sustained release	82.21 after 48 h	This study
Poly(ether-ester) urethane acrylates (Pdiol2000-IPDI)	Solution: phosphate buffer saline (PBS)	High level of drug release observed in the first 100 h, and prolonged release over 200 h,	87 after 250 h	Feng et al. (2017)
Poly (lactic-co-glycolic acid)	pH 7.4 in PBS solution at temperature of 37 °C	27.9% of the drug was released in 30 min, 75% was released after 6 h	89.3 after 48 h	Li et al. (2017)
Curdlan – polyethylene oxide	pH 7.4 in PBS solution at temperature of 37 °C	62% of the drug was released in 2 h, followed by a slower and more gradual tetracycline release pattern	~100% at 5.5 h	El-Naggar, Abdelgawad, Salas and Rojas (2016)
Solid lipid microparticles	pH 7.4 in PBS solution at temperature of 37 °C	High burst release values (more than 35%) in the first 20 min followed by gradual tetracycline release pattern	97.0 ± 4.2 after 24 h	Rahimpour, Javadzadeh and Hamishehkar (2016)

is consistent with the experimental data and its specific characteristic.

3.3. Tetracycline release study

The release of tetracycline from CNC was influenced by pH condition of the PB mediums (2.1 and 7.2) also the interaction between tetracycline and the ionic components in the PB solutions. Since the release of tetracycline from CNC – tetracycline complex (Eqs. (5) and (6)) involving dissociation of CNC – tetracycline complex into protonated or deprotonated tetracycline, therefore, the kinetic release of tetracycline into PB solutions, follows the second order of reaction (Lin, Qiao, Yu, Ismadji & Lu, 2009)

$$\frac{dC_{TC}}{dt} = k(C_{TCe} - C_{TC})^2 \quad (7)$$

where C_{TC} is the concentration of tetracycline in the PB solution at any time, k is a constant, and C_{TCe} is a concentration of tetracycline in the PB solutions at equilibrium condition. Initial concentration of tetracycline in PB solutions $C_{TCo} = 0$ and when it is integrated into Eq. (7) gives the following equation:

$$C_{TC} = \frac{C_{TCe}^2.k.t}{(1 + C_{TCe}.k.t)} \quad (8)$$

Parameters C_{TCe} and k obtained from the kinetic adsorption experimental data, which can be well fitted into Eq. (8). The values of parameter C_{TCe} and k at pH 7.2 are 101.95 mg/L and 0.004 L/mg s, respectively. While at pH 2.1 the values of parameter C_{TCe} and k are 35.26 mg/L and 0.0018 L/mg.s.

At pH 7.2 (neutral condition), tetracycline was rapidly released within the first 10 h followed by a sustained release until the equilibrium condition was reached (Fig. 7). Approximately 80% of tetracycline adsorbed on the CNC was released into PB (7.2) solution in 10 h (C_{TC} = 82.49 mg/L). The maximum tetracycline release was approximately 82.21% after the equilibrium condition between CNC and PB (7.2) solution was achieved within 48 h (C_{TCe} = 99.89 mg/L).

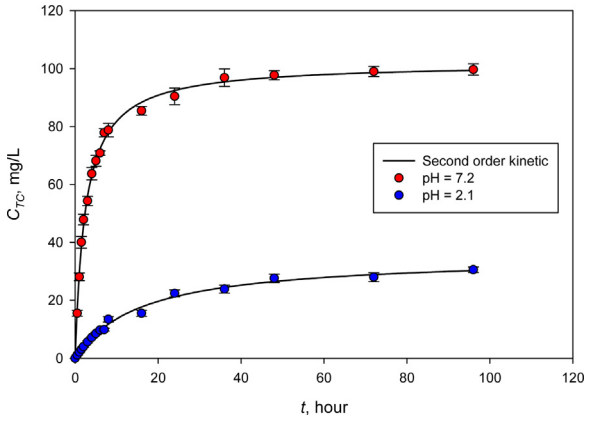

Fig. 7. Tetracycline release behavior at pH 7.2 and pH 2.1.

An opposite phenomenon was observed for tetracycline release at PB medium with acidic pH of 2.1 (Fig. 7). In this acidic condition, the maximum amount of tetracycline release (25.1% of the initial amount) was much lower compare to neutral condition (pH 7.2).

The pH condition of release medium (acid/neutral/basic) plays a major role in controlling the release rate of tetracycline from CNC. In general, our observations show that CNC is negatively charged (−22 to −25 mV) over the studied pH range, whereas tetracycline exist in three different ionic forms (cations, zwitterions, and anions). At pH < 3.3, the tetracycline molecules was positively charged, while the CNC was negatively charged, thus in the PB solution of pH 2.1 the electrostatic interaction between CNC and tetracycline was much stronger than the interaction of tetracycline and the solvent. At pH 7.2, tetracycline molecules serve as zwitterions that carry no net electrical charge and resulted in a reduced electrostatic interaction between CNC and tetracycline (Yu, Ma & Han, 2014). Furthermore, at neutral pH the hydrophilicity of tetracycline also increases, these phenomena enhanced the release of tetracycline to the PB solu-

tion. Comparison of tetracycline release efficiency between CNC and other drug carriers is given in Table 3.

It can be seen (Table 3) that several synthetic drug carriers (Poly (lactic-co-glycolic acid), solid lipid microparticles) and CNC have high tetracycline release pattern at early stage of drug release experiments. This high release values indicates that some of the tetracycline molecules were adsorbed in the surface of adsorbent with low adsorption affinity; therefore, the tetracycline molecules were easily released or desorbed to the PB solution during the first hour of the experiments. CNC has comparable value of release efficiency with poly (lactic-co-glycolic acid) especially after 6 h of release study (CNC around 72% and poly (lactic-co-glycolic acid) around 75%). Comparing to curdlan – polyethylene oxide composite, the tetracycline release efficiency of CNC after 2 h was lower (48%). This phenomenon indicates that CNC has stronger adsorption affinity than curdlan – polyethylene oxide composite. With high release efficiency (>80%), CNC has potential application as drug carrier.

4. Conclusion

Passionfruit peels (PP) can serve as potential precursor for their conversion into CNC. The maximum yield of CNC extracted from the pre-treated pulp of PP was 58.1 ± 1.7%. The adsorption of tetracycline on CNC were conducted at varied pH 3–7 with the optimum uptake of tetracycline was achieved at pH 3. The most widely used isotherm equations of Langmuir and Freundlich were employed to fit the adsorption experimental data, where Langmuir could better represent the data than Freundlich equation. The drug release study was conducted at two different pH of phosphate buffer solutions (7.2 and 2.1) with the maximum release of tetracycline at pH 7.2 was 82.21% and at pH 2.1 was 25.1%. The second order kinetic model could represent the release data well.

Acknowledgements

The authors gratefully acknowledge the financial support from Indonesia Ministry of Research and Technology and Higher Education through Fundamental Research Grant 2016–2017.

References

Bano, S., & Negi, Y. S. (2017). Studies on cellulose nanocrystals isolated from groundnut shells. *Carbohydrate Polymers*, *157*, 1041–1049.

Barana, D., Salanti, A., Orlandi, M., Ali, D. S., & Zoia, L. (2016). Biorefinery process for the simultaneous recovery of lignin, hemicallulose: Cellulose nanocrystals and silica from rice husk and *Arundo donax*. *Industrial Crops and Products*, *86*, 31–39.

Brinchi, L., Cotana, F., Fortunati, E., & Kenny, J. M. (2013). Production of nanocrystalline cellulose from lignocellulosic biomass: Technology and applications. *Carbohydrate Polymers*, *94*, 154–169.

Carrier, M., Loppinet-Serani, A., Denux, D., Lasnier, J. M., Ham-Pichavant, F., Cansell, F., et al. (2011). Thermogravimetric analysis as a new method to determine the lignocellulosic composition of biomass. *Biomass and Bioenergy*, *35*, 298–307.

Cherian, B. M., Leão, A. L., De Souza, S. F., Thomas, S., Pothan, L. A., & Kottaisamy, M. (2010). Isolation of nanocellulose from pineapple leaf fibres by steam explosion. *Carbohydrate Polymers*, *81*, 720–725.

Coates, J. (2006). *Interpretation of Infrared Spectra, A Practical Approach Encyclopedia of Analytical Chemistry*. John Wiley & Sons.

Ditzel, F. I., Prestes, E., Carvalho, B. M., Demiate, I. M., & Pinheiro, L. A. (2017). Nanocrystalline cellulose extracted from pinewood and corncob. *Carbohydrate Polymers*, *157*, 1577–1585.

El-Naggar, M. E., Abdelgawad, A. M., Salas, C., & Rojas, O. J. (2016). Curdlan in fibers as carriers of tetracycline hydrochloride: Controlled release and antibacterial activity. *Carbohydrate Polymers*, *154*, 194–203.

Feng, X., Wang, G., Neumann, K., Yao, W., Ding, L., Li, S., et al. (2017). Synthesis and characterization of biodegradable poly(ether-ester) urethane acrylates for controlled drug release. *Materials Science and Engineering C*, *74*, 270–278.

Garcia, A., Labidi, J., Belgacem, M. N., & Bras, J. (2017). The nanocellulose biorefinery: Woody versus herbaceous agricultural wastes for NCC production. *Cellulose*, *24*, 693–704.

Haafiz, M. K. M., Eichhorn, S. J., Hassan, A., & Jawaid, M. (2013). Isolation and characterization of microcrystalline cellulose from oil palm biomass residue. *Carbohydrate Polymers*, *93*, 628–634.

Jackson, J. K., Letchford, K., Wasserman, B. Z., Ye, L., Hamad, W. Y., & Burt, H. M. (2011). The use of nanocrystalline cellulose for the binding and controlled release of drugs. *International Journal of Nanomedicine*, *6*, 321–330.

Lam, E., Male, K. B., Chong, J. H., Leung, A. C. W., & Luong, J. H. T. (2012). Applications of functionalized and nanoparticle-modified nanocrystalline cellulose. *Trend in Biotechnology*, *30*, 283–290.

Li, R., Fei, J., Cai, Y., Li, Y., Feng, J., & Yao, J. (2009). Cellulose whiskers extracted from mulberry: A novel biomass production. *Carbohydrate Polymers*, *76*, 94–99.

Li, T., Ding, X., Tian, L., Hu, J., Yang, X., & Ramakrishna, S. (2017). The control of beads diameter of bead-on-string electrospun nanofibers and the corresponding release behaviors of embedded drugs. *Materials Science and Engineering C*, *74*, 471–477.

Lin, N., & Dufresne, A. (2014). Nanocellulose in biomedicine: Current status and future prospect. *European Polymer Journal*, *59*, 302–325.

Lin, C. X., Qiao, S. Z., Yu, C. Z., Ismadji, S., & Lu, G. Q. (2009). Periodic mesoporous silica and organosilica with controlled morphologies as carriers for drug release. *Microporous and Mesoporous Materials*, *117*, 213–219.

Lu, P., & Hsieh, Y. L. (2012). Cellulose isolation and core-shell nanostructures of cellulose nanocrystals from chardonnay grape skins. *Carbohydrate Polymers*, *87*, 2546–2553.

Mandal, A., & Chakrabarty, D. (2011). Isolation of nanocellulose from waste sugarcane bagasse (SCB) and its characterization. *Carbohydrate Polymers*, *86*, 1291–1299.

Morelli, C. L., Marconcini, J. M., Pereira, F. V., Bretas, R. E. S., & Branciforti, M. C. (2012). Extraction and characterization of cellulose nanowhiskers from balsa wood. *Macromolecular Symposia*, *319*, 191–195.

Nascimento, D. M. D., Almeida, J. S., Vale, M. D. S., Leitao, R. C., Muniz, C. R., Figueiredo, M. C. B. D., et al. (2016). A comprehensive approach for obtaining cellulose nanocrystal from coconut fiber: part I: Proposition of technological pathways. *Industrial Crops and Products*, *93*, 66–75.

Qing, W., Wang, Y., Wang, Y. Y., Zhao, D., Liu, X., & Zhu, J. (2016). The modified nanocrystalline cellulose for hydrophobic drug delivery. *Applied Surface Science*, *366*, 404–409.

Rahimpour, Y., Javadzadeh, Y., & Hamishehkar, H. (2016). Solid lipid microparticles for enhanced dermal delivery of tetracycline HCl. *Colloids and Surfaces B: Biointerfaces*, *145*, 14–20.

Sarma, S. J., Ayadi, M., Brar, S. K., & Berry, R. (2017). Sustainable commercial nanocrystalline cellulose manufacturing process with acid recycling. *Carbohydrate Polymers*, *156*, 26–33.

Shamskar, K. R., Heidari, H., & Rashidi, A. (2016). Preparation and evaluation of nanocrystalline cellulose aerogels from raw cotton and cotton stalk. *Industrial Crops and Products*, *93*, 203–211.

Sigma-Aldrich. (2013). *MSDS cetyltrimethylammonium bromide. version 5.2*. [Revision Date 16.11.2012].

Silvério, H. A., Flauzino, N. W. P., Dantas, N. O., & Pasquini, D. (2013). Extraction and characterization of cellulose nanocrystals from corncob for application as reinforcing agent in nanocomposites. *Industrial Crops and Products*, *44*, 427–436.

Sim, S. F., Mohamed, M., Lu, N. A. L. M. I., Sarman, N. S. P., & Samsudin, S. N. S. (2012). Computer-assisted analysis of Fourier Transform Infrared (FTIR) spectra for characterization of various treated and untreated agriculture biomass. *Bioresources*, *7*, 5367–5380.

Sun, B., Hou, Q., He, Z., Liu, Z., & Ni, Y. (2014). Cellulose nanocrystals (CNC) as carriers for a spirooxazine dye and its effect on photochromic efficiency. *Carbohydrate Polymers*, *111*, 419–424.

Todorciuc, T., Capraru, A. M., Kratochvilova, I., & Popa, V. I. (2009). Characterization of non-wood lignin and its hydroxymethylated derivatives by spectroscopy and self-assembling investigation. *Cellulose Chemistry and Technology*, *43*, 399–408.

Yu, F., Ma, J., & Han, S. (2014). Adsorption of tetracycline from aqueous solutions onto multi-walled carbon nanotubes with different oxygen contents. *Scientific Report*, *4*, 5326.

Zainuddin, N., Ahmad, I., Kargarzadeh, H., & Ramli, S. (2017). Hydrophobic kenaf nanocrystalline cellulose for the binding of curcumin. *Carbohydrate Polymers*, *163*, 261–269.